

Effect of Monomer Loading and Pressure on Particle Formation in Nitroxide-Mediated Precipitation Polymerization in Supercritical Carbon Dioxide

Padraig O'Connor,[†] Per B. Zetterlund,^{*,‡} and Fawaz Aldabbagh^{*,†}

[†]*School of Chemistry, National University of Ireland, Galway, Ireland, and* [‡]*Centre for Advanced Macromolecular Design (CAMD), School of Chemical Sciences and Engineering, The University of New South Wales, Sydney NSW 2052, Australia*

Received October 6, 2009; Revised Manuscript Received November 6, 2009

ABSTRACT: The critical degree of polymerization (J_{crit}) at which polymer chains become insoluble in the continuous medium and particle formation commences has been estimated under a variety of experimental conditions for the nitroxide-mediated precipitation polymerizations of styrene (St) at 110 °C and *tert*-butyl acrylate (*t*-BA) at 118 °C in supercritical carbon dioxide (scCO₂) mediated by *N*-*tert*-butyl-*N*-[1-diethylphosphono(2,2-dimethylpropyl)]oxy (SG1). The value of J_{crit} increases with increasing target molecular weight, initial monomer loading, and pressure. Under the conditions investigated, J_{crit} for *t*-BA is higher than that for St, which is consistent with greater solubility of poly(acrylates) in neat scCO₂. A simple graphical approach has been developed and successfully employed, whereby J_{crit} can be predicted as a function of both target molecular weight and initial monomer loading on the basis of a data set of J_{crit} versus initial monomer loading.

Introduction

Supercritical carbon dioxide (scCO₂) is a benign reaction solvent well-suited for heterogeneous radical polymerizations because most organic small molecules (incl. monomer, initiator) are soluble in the medium, but the resulting high molecular weight (MW) polymers are insoluble.^{1,2} Polymer chains are soluble in the medium up to a certain critical degree of polymerization (J_{crit}) when chains become insoluble and precipitate, resulting in particle formation. At J_{crit} , the polymerization changes from a homogeneous phase in scCO₂ to a heterogeneous system. Dispersion polymerizations contain a colloidal stabilizer to prevent coagulation of particles giving polymer of narrow particle size distributions and more well-defined particles ($d \approx 100$ nm to 15 μm).^{1–3}

Over the past 20 years, controlled/living radical polymerization (CLRP) has revolutionized polymer chemistry, allowing the synthesis of narrow molecular weight distribution (MWD) polymer, as well as complex architectures under less stringent polymerization conditions than ionic methods.⁴ Although initially most CLRPs were carried out under homogeneous conditions, many have since been carried out using commercially important heterogeneous techniques.^{5,6} The three most widely used CLRPs, nitroxide-mediated radical polymerization (NMP),^{7–12} atom transfer radical polymerization (ATRP),^{13–18} and reversible addition–fragmentation chain transfer (RAFT)^{19–22} have all been successfully implemented as heterogeneous polymerizations in scCO₂. However, only NMP has thus far been shown to proceed in a controlled/living manner to high conversion using the stabilizer-free precipitation system.^{10–12} Furthermore, under certain conditions (70% w/v monomer, [SG1]₀/[AIBN]₀ = 1.99, 110 °C, 30 MPa, where the nitroxide is SG1 = *N*-*tert*-butyl-

N-[1-diethylphosphono(2,2-dimethylpropyl)]oxy and AIBN = 2,2'-azobisisobutyronitrile), we showed that the precipitation NMP of styrene (St) can proceed with better control over the MWD than the corresponding solution polymerization.^{11,12}

The slow build up in MW in a CLRP by virtue of the equilibrium between active (propagating radicals) and dormant polymer chains allows measurement of J_{crit} by estimating via visual observation the conversion (and thus the MW) at which the reaction mixture changes from transparent to opaque (the cloud point). In a conventional nonliving polymerization, the system would immediately become heterogeneous because of the instantaneous formation of high MW polymer. The value of J_{crit} would change with conversion as the composition of the continuous phase changes because chains are continuously initiated and grow to reach J_{crit} throughout the polymerization. However, in CLRP, the initial stoichiometry dictates the conversion at J_{crit} , and a single J_{crit} value applies to a given polymerization system. This technique has been employed to estimate J_{crit} for precipitation/dispersion NMP of St in scCO₂.^{8,11}

To date, only the NMP of St in scCO₂ has been studied, and no information on controlled/living character at low conversion (before J_{crit}), when the reaction is homogeneous, has been obtained. The NMP of St and *tert*-butyl acrylate (*t*-BA) in scCO₂ before and after J_{crit} is now presented. The detailed effects of composition and pressure on J_{crit} and the associated controlled/living character are examined. This has led us to develop a simple graphical approach to predicting J_{crit} as a function of both target MW ([monomer]₀/[initiator]₀) and initial monomer loading based on a data set of J_{crit} versus initial monomer loading. These findings will enable future optimization of heterogeneous (precipitation and dispersion) CLRPs in scCO₂.

Experimental Section

Materials. St (Aldrich, > 99%) and *t*-BA (Aldrich, 98%) were distilled under reduced pressure before use. AIBN (DuPont

*Corresponding authors. (P.B.Z.) Tel: +61-2-9385 4331. Fax: +61-2-9385 6250. E-mail: p.zetterlund@unsw.edu.au. (F.A.) Tel: +353-91-493120. Fax: +353-91-525700. E-mail: fawaz.alabbagh@nuigalway.ie.

Table 1. Results for Measurement of J_{crit} for Poly(styrene) using Different Monomer Loadings and Pressures at 110 °C

$[M]_0$ (% w/v) ^a	pressure (MPa)	time at J_{crit} (min)	conv. (%)	M_n	$M_{n,\text{th}}$	M_w/M_n	J_{crit}
80	30	272	32.8	13 450	13 100	1.13	129
70	30	227	22.0	8550	8800	1.15	82
60	30	119	14.1	5000	5650	1.17	48
55	30	96	10.3	4250	4100	1.18	41
50	30	71	8.4	3450	3400	1.17	33
40	30	51	3.9	3000	1550	1.18	29
35	30	44	1.8	2950	700	1.19	28
30	30	35	0.9	2800	350	1.35	27
70	23	264	21.9	7600	8750	1.20	73
70	15	175	16.0	6100	6400	1.22	59
70	10	140	16.8	5400	6700	1.21	52

^a Initial monomer loading.

Chemical Solution Enterprise) was recrystallized from methanol before use. SG1 (also known as DEPN) was prepared according to the literature²³ with purity (96%) determined using ¹H NMR spectroscopy from the reaction of SG1 radical with pentafluorophenylhydrazine (Aldrich). Reagent grade toluene (Aldrich, ≥ 99.7%), methanol (Corcoran Chemicals, 99.9%), dichloromethane (Corcoran Chemicals, 99.9%), and CO₂ (BOC, 99.8%) were used as received. Macroinitiator (poly(St)-T, PSt-T: where, T = SG1, $M_n = 4250 \text{ g mol}^{-1}$, $M_w/M_n = 1.18$) was obtained from the J_{crit} measurement experiment at 55% monomer loading. (See Table 1.)

Equipment and Measurements. All NMP in scCO₂ were conducted in a 100 mL stainless steel Thar reactor with 180° inline sapphire windows and overhead Magdrive stirrer with maximum programmable operating pressure and temperature of 41.4 MPa and 120 °C, respectively. The pressure was produced and maintained by a Thar P-50 series high-pressure pump to within ±0.2 MPa. The temperature was regulated by a Thar CN6 controller to within ±1 °C. The reactor is connected to a Thar automated back pressure regulator (ABPR, a computer-controlled needle valve) for controlled venting.

M_n and polydispersity (M_w/M_n) were determined using a gel permeation chromatography (GPC) system consisting of a Viscotek DM 400 data manager, a Viscotek VE 3580 refractive-index detector, and two Viscotek Viscogel GMH_{HR}-M columns. Measurements were carried out using tetrahydrofuran (THF) at a flow rate of 1.0 mL·min⁻¹ at 35 °C with columns calibrated using 12 linear poly(St) standards ($M_n = 162\text{--}6035000$). M_n and M_w/M_n values for poly(*t*-BA) (Pr-BA) are not accurate because of the calibration against PSt standards. However, our primary focus is trends as well as shape and relative position of MWDs. M_n is given in grams per mole (g·mol⁻¹) throughout to the nearest 50 g·mol⁻¹.

Polymerization of St in scCO₂. The reactor was loaded with St (58.320 g, 0.56 mol), PSt-T (1.680 g, 0.40 mmol) (60% w/v includes St + PSt-T), and SG1 (47 mg, 0.16 mmol). The reactor was sealed with the magnetically coupled stirring lid (Magdrive). The mixture was purged for 15 min by bubbling gaseous CO₂ through the mixture to remove air. Liquid CO₂ (~5 MPa) was added, and the temperature was raised to the reaction temperature of 110 °C, followed by the pressure to the reaction pressure (in this case 30 MPa) by the addition of CO₂. The transparent reaction mixture was stirred at ~1000 rpm throughout and monitored through the inline sapphire windows, and if J_{crit} was required, stopped when the reaction mixture became opaque. Heating was stopped, and rapid external cooling using dry ice was carried out (this caused the temperature of the reactor to drop to ~80 °C in 10 min). The CO₂ was vented slowly from the reactor (when at approximately room temperature after 40 min of cooling) through a suitable solvent (methanol) to prevent the loss of polymer and opened using the ABPR, and the reaction mixture pipetted directly from the reactor. The polymer was precipitated from excess methanol, filtered, and dried prior to conversion measurement by gravimetry.

Table 2. Results for Measurement of J_{crit} for Poly(*tert*-butyl acrylate) using Different Monomer Loadings and Pressures at 118 °C

$[M]_0$ (% w/v) ^a	pressure (MPa)	time at J_{crit} (min)	conv. (%)	M_n	$M_{n,\text{th}}$	M_w/M_n	J_{crit}
70	30	1159	66.0	17100	17750	1.44	133
60	30	960	51.8	12650	13950	1.37	99
50	30	720	38.8	10500	10500	1.28	82
30	30	225	10.0	3900	2700	1.29	30
60	23	576	43.1	11100	11600	1.35	87
60	15	428	29.6	9500	8000	1.29	74
60	10	335	24.7	7750	6650	1.23	61

^a Initial monomer loading.

Polymerization of *t*-BA in scCO₂. *t*-BA (50.000 g, 0.39 mol, 50% w/v), AIBN (0.124 g, 0.76 mmol) and SG1 (0.550 g, 1.87 mmol) were heated at 118 °C and 30 MPa using the polymerization procedure above. The polymer was precipitated from a 3:2 water/methanol mixture, filtered, and dried prior to conversion measurement by gravimetry.

Measurement of J_{crit} in scCO₂. For the 70% w/v initial St loading and $M_{n,\text{th}}$ at 100% conversion = 40 000 (eq 1), St (70.000 g, 0.67 mol), AIBN (0.173 g, 1.05 mmol), and SG1 (0.620 g, 2.11 mmol) were heated at 110 °C and 30 MPa, and the polymerization stopped at J_{crit} (see procedure above). The theoretical value of M_n ($M_{n,\text{th}}$) is calculated via eq 1

$$M_{n,\text{th}} = \frac{\alpha[M]_0 MW_{\text{mon}}}{2f[\text{AIBN}]_0} \quad (1)$$

where f is the AIBN initiator efficiency, α is the fractional conversion of monomer, $[M]_0$ is the initial monomer concentration, and MW_{mon} is the molecular weight of the monomer. The value of f in scCO₂ at 59.4 °C has been estimated to be 0.83 by DeSimone and coworkers.²⁴ In the present study, f was estimated by fitting the initial portion of the M_n versus conversion plots of the polymerization data to yield $f = 0.83$ (St) and 1.23 (*t*-BA). $M_{n,\text{th}}$ values were computed throughout this work using eq 1 in connection with these f -estimates. A value of f greater than unity, as obtained for *t*-BA, is of course not physically meaningful; this is most likely a result of accumulated error primarily due to inaccuracy caused by the use of linear PSt standards. The initiator efficiency of the macroinitiator PSt-T is taken as 1.

Chain Extension of Pr-BA with Bulk St. Pr-BA macroinitiator from 70% w/v initial loading experiment (Table 2) (0.4270 g, 0.025 mmol), St (2 g, 19.20 mmol), and SG1 (1.5 mg, 5.10 μmol) were charged in a glass ampule. Air was removed by several freeze–thaw degas cycles before the ampule was sealed. It was then placed in an aluminum heating block at 120 °C for 24 h. The polymerization was quenched by immersing the ampule into an ice–water bath. Subsequently, the mixture was dissolved in dichloromethane and poured into an excess of 3:2 water/methanol to precipitate the formed polymer. After filtration and drying, the conversion was obtained from the increase in weight of polymeric material.

Results and Discussion

NMP of St and *t*-BA in scCO₂. Conversion–time and MWD data for NMP of St (60% w/v) in scCO₂ initiated by a soluble macroinitiator (PSt-T, where T = SG1, with 40 mol % free SG1 relative to PSt-T; the addition of free SG1 is primarily to alleviate partitioning effects⁸ anticipated after J_{crit}) at 110 °C and 30 MPa are displayed in Figures 1 and 2. The polymerization proceeded to intermediate conversion with no sign of having reached a limiting conversion (Figure 1), and the MWDs shifted to higher MW with increasing conversion (Figure 2).

We obtained the value of J_{crit} by visually monitoring the polymerization via the reactor inline sapphire windows. The

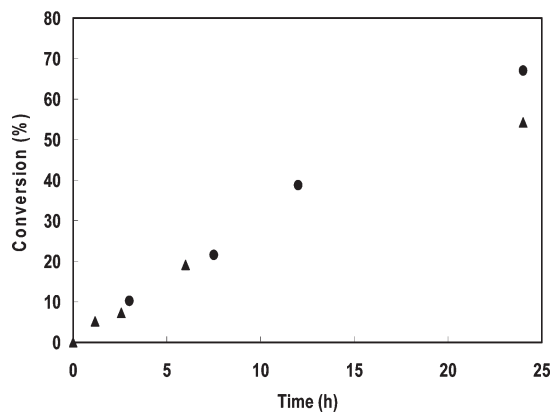


Figure 1. Conversion versus time for the SG1-mediated polymerization of St (\blacktriangle , 60% w/v) at 110 °C (initiated by PSt-T macroinitiator in the presence of 40 mol % free SG1) and *t*-BA (\bullet , 50% w/v) at 118 °C ($[SG1]_0/[AIBN]_0 = 2.5$) in $scCO_2$ at 30 MPa. J_{crit} is at 7.3 and 38.8% conversion for St and *t*-BA, respectively.

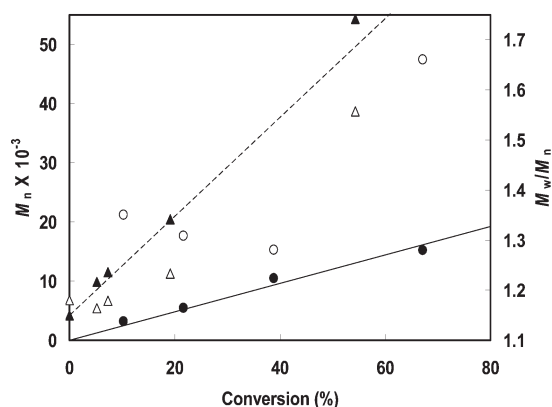


Figure 2. M_n (closed symbols) and M_w/M_n (open symbols) versus conversion for the SG1-mediated polymerization of St (\blacktriangle , \triangle , 60% w/v) at 110 °C (initiated by PSt-T macroinitiator in the presence of 40 mol % free SG1) and *t*-BA (\bullet , \circ , 50% w/v) at 118 °C ($[SG1]_0/[AIBN]_0 = 2.5$) in $scCO_2$ at 30 MPa. Dashed and continuous lines represent $M_{n,th}$ for St and *t*-BA polymerizations, respectively. J_{crit} is at 7.3 and 38.8% conversion for St and *t*-BA, respectively.

polymerization was stopped at the point when the mixture changed from transparent to opaque. Subsequent measurement of M_n yielded $J_{crit} = 110$ ($M_n = 11450$) at 7.3% conversion. Because of the inherent polydispersity of the polymer (despite the CLRP process), this value of J_{crit} is to an extent an underestimate of the true J_{crit} . This is because the chains of the highest MW of the MWD will be the ones that first precipitate, whereas the obtained J_{crit} corresponds to the full MWD. The values of M_w/M_n increased with conversion in the range of 1.16 to 1.18 before J_{crit} and 1.23 to 1.56 after J_{crit} (Figure 2), indicating good control/livingness in agreement with our previously reported SG1/AIBN-initiated precipitation polymerizations.^{10–12}

Conversion–time and MWD data for NMP of *t*-BA (50% w/v) in $scCO_2$ initiated by AIBN and controlled using an excess of nitroxide, $[SG1]_0/[AIBN]_0 = 2.5$, at 118 °C and 30 MPa are displayed in Figures 1 and 2. Similarly to the St NMP above, M_n increased linearly with conversion, which is indicative of good controlled/living character, and $J_{crit} = 82$ ($M_n = 10510$) was recorded at 38.8% conversion. M_w/M_n increased dramatically after J_{crit} (1.28 to 1.35 before J_{crit} and 1.66 after J_{crit}), which is probably the consequence of a lowering in the free $[SG1]$ at the locus of polymerization due to partitioning toward the $scCO_2$ continuous phase

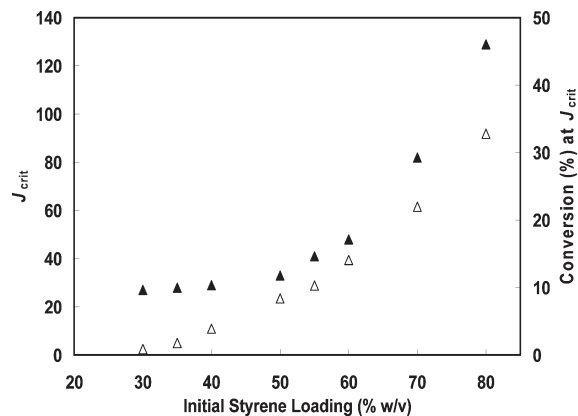


Figure 3. J_{crit} (\blacktriangle) and conversion at J_{crit} (\triangle) versus initial St loading for the SG1-mediated polymerization of St in $scCO_2$ at 110 °C and 30 MPa ($[SG1]_0/[AIBN]_0 = 2.0$, theoretical M_n at 100% conversion ($M_{n,th} = 40000$)).

(the particle phase is the main locus of polymerization after J_{crit}),^{2,12} although partial loss of control of NMP would be expected at high conversions.

Effect of Monomer Loading on J_{crit} . Values of J_{crit} were estimated for the NMP of St in $scCO_2$ at a range of different initial monomer loadings of 30–80% w/v using $[SG1]_0/[AIBN]_0 = 2.0$ ($M_{n,th} = 40000$ at 100% conversion) at 110 °C and 30 MPa (Figure 3, Table 1). As expected, J_{crit} increased with monomer loading because of the increased solubility of the polymer in the increasingly monomer-rich continuous phase. However, J_{crit} increased only slightly from 27 (conv. = 0.9%) to 33 (conv. = 8.4%) as the initial loading was increased from 30 to 50% w/v. As the monomer loading was increased further to 55% w/v ($J_{crit} = 41$, conv. = 10.3%), the values of J_{crit} increased more dramatically to reach 129 (conv. = 32.8%) at 80% w/v.

Considering that the ratio $[St]_0/[AIBN]_0$ was the same in all polymerizations, one would expect that M_n versus conversion of these polymerizations would give a straight line (provided that f does not change significantly with monomer loading); that is, J_{crit} versus conversion at J_{crit} should give a straight line. It is, however, apparent from Figure 3 (and Table 1) that at low monomer loadings, this is not the case; J_{crit} is higher than expected considering the conversions at J_{crit} . Because of the short polymerization times required to reach J_{crit} (35–51 min at 30–40% w/v St, Table 1), some fraction of AIBN remains undecomposed at J_{crit} , thus giving $M_n > M_{n,th}$. Estimation of apparent f values based on eq 1 gives $f \approx 0.1$, 0.4, and 0.78 at 30, 40, and 50% w/v St, respectively, with $M_n \approx M_{n,th}$ at 50% w/v St. This hypothesis was confirmed by taking a 35% w/v initial loading polymerization of St (under the same conditions as that used for the J_{crit} measurement, where apparent $f = 0.2$) to well beyond J_{crit} (15 h), which gave $M_n = 13700$ ($M_w/M_n = 1.33$) at 31.3% conversion. This approached the $M_{n,th} = 12500$ with apparent $f \approx 0.76$, which is close to the literature value of 0.83.²⁴

Values of J_{crit} were estimated for the NMP of *t*-BA in $scCO_2$ at a range of different initial monomer loadings of 30–70% w/v using $[SG1]_0/[AIBN]_0 = 2.5$ ($M_{n,th} = 26,900$ at 100% conversion) at 118 °C and 30 MPa (Figure 4, Table 2). J_{crit} and the conversion at J_{crit} increased almost linearly with initial monomer loading from $J_{crit} = 30$ at 10.0% to 133 at 66.0% conversion, which is indicative of increased polymer solubility in the continuous phase. The J_{crit} (and conversion at J_{crit}) values for *t*-BA (for a given monomer loading) are considerably higher than those for St, indicating greater

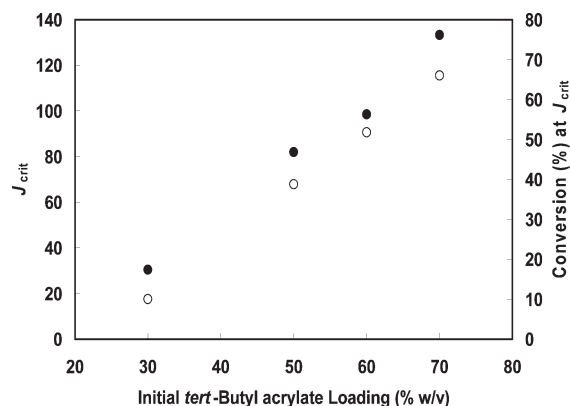


Figure 4. J_{crit} (●) and conversion at J_{crit} (○) versus initial *t*-BA loading for the SG1-mediated polymerization of *t*-BA in scCO_2 at 118 °C and 30 MPa ($[\text{SG1}]_0/[\text{AIBN}]_0 = 2.5$, theoretical M_n at 100% conversion ($M_{n,\text{th}} = 26\,900$)).

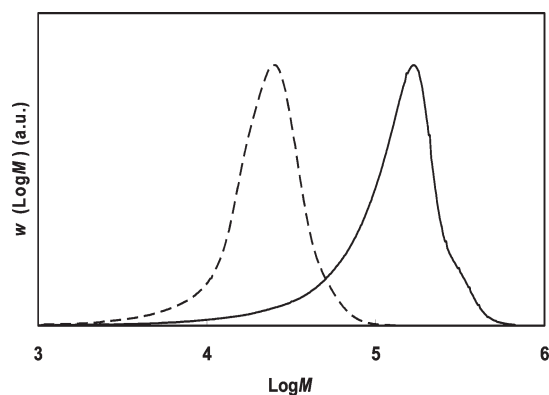


Figure 5. MWDs (normalized to peak height) of the chain extension of Pt-BA (from 70% w/v initial monomer loading experiment (Table 2) $M_n = 17\,100$, $M_w/M_n = 1.44$) with bulk St at 120 °C to give Pt-BA-*b*-PSt; $M_n = 65\,200$, $M_w/M_n = 2.23$, Conv. = 91.1%.

solubility of Pt-BA compared with PSt in scCO_2 at the respective temperatures and pressures. The St and *t*-BA polymerizations resulted in similar M_n vs conversion plots (Table 1 and 2); that is, similar M_n values were reached at a given conversion, thus making direct comparison meaningful in this sense. It has been reported that the solubility of poly(butyl acrylate) in neat scCO_2 is higher than that of PSt, mainly as a result of the higher glass-transition temperature of PSt.²⁵

Longer polymerization times were required to reach J_{crit} for *t*-BA than St (Tables 1 and 2) and the temperature was higher for *t*-BA (118 vs 110 °C); therefore, partial decomposition of AIBN at J_{crit} at low monomer loadings was not an issue for *t*-BA (i.e., J_{crit} increases close to linearly with conversion at J_{crit}). Controlled/living character was maintained up to high conversion, as indicated by $M_n = 17\,100$ remaining close to $M_{n,\text{th}} = 17\,750$ at 66.0% conversion (Table 2) and confirmed by efficient chain extension of this sample with bulk St (Figure 5).

The J_{crit} values for St appear to be consistent with the work of Vana and coworkers, who reported homogeneous RAFT polymerizations of St in scCO_2 at 80 °C and 30 MPa using 78% vol % St for $M_n < 29\,800$.²⁶

Predicting J_{crit} . The J_{crit} data described above for St and *t*-BA can be employed to predict J_{crit} under different experimental conditions in terms of the targeted MW ($M_{n,\text{th}}$ at 100% conversion) and the initial monomer loading for the systems investigated (i.e., same temperature and pressure).

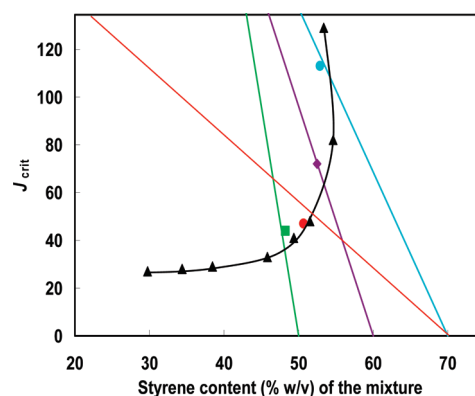


Figure 6. Plot of J_{crit} versus St content of the mixture at J_{crit} (▲) for the SG1-mediated polymerization of St in scCO_2 at 110 °C and 30 MPa ($[\text{SG1}]_0/[\text{AIBN}]_0 = 2.0$; $M_{n,\text{th}}$ (100% conv.) = 40 000). The straight lines (colors), each represent a given set of conditions in terms of initial monomer loading and $M_{n,\text{th}}$, describing how the degree of polymerization changes with the % w/v monomer content when the polymerization proceeds in accordance with eq 1. $M_{n,\text{th}}$ lines: 70% w/v St, $M_{n,\text{th}} = 20\,000$ (●; red), 70% w/v St, $M_{n,\text{th}} = 50\,000$ (●; blue), 60% w/v St, $M_{n,\text{th}} = 60\,000$ (◆; purple), and 50% w/v St, $M_{n,\text{th}} = 100\,000$ (■; green). $M_{n,\text{th}}$ values in the legend refer to 100% conversion, and symbols represent individual experiments carried out using these conditions.

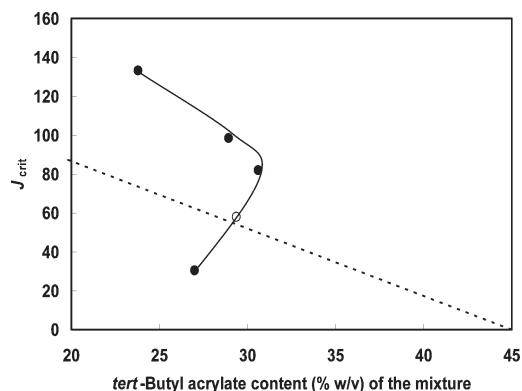


Figure 7. Plot of J_{crit} versus *t*-BA content of the mixture at J_{crit} (●) for the SG1-mediated polymerization of *t*-BA in scCO_2 at 118 °C and 30 MPa ($[\text{SG1}]_0/[\text{AIBN}]_0 = 2.5$, $M_{n,\text{th}}$ (100% conv.) = 26 900). The straight dotted line represents a given set of conditions in terms of initial monomer loading and $M_{n,\text{th}}$ and describes how the degree of polymerization changes with the % w/v monomer content when the polymerization proceeds in accordance with eq 1. $M_{n,\text{th}}$ line: 45% w/v *t*-BA, $M_{n,\text{th}} = 20\,000$ at 100% conversion, and (○) represents the J_{crit} experiment using these conditions.

For example, if the ratio of monomer to AIBN is altered (i.e., different $M_{n,\text{th}}$) but the initial monomer loading is the same, then how does J_{crit} change? To this end, the J_{crit} data are presented graphically in Figures 6 and 7 in the form of a plot of J_{crit} versus the monomer content (as % w/v) of the mixture at J_{crit} (readily calculated from the monomer conversion at J_{crit}). The J_{crit} value can be graphically predicted by constructing theoretical lines of $M_{n,\text{th}}$ from the initial monomer loading based on eq 1. The theoretical lines describe how the degree of polymerization changes with the % w/v monomer remaining when the polymerization proceeds in accordance with eq 1. J_{crit} of the “new” system corresponds to the point of intersection of the straight $M_{n,\text{th}}$ line and the J_{crit} curve. In the case of St (Figure 6, Table 3), using 70% w/v initial St loading and $M_{n,\text{th}} = 20\,000$ and 50 000 (at 100% conv.), the predictive graphical approach resulted in $J_{\text{crit}} = 50$ and 110 (at the intersections), respectively, which are remarkably close to the experimentally (in independent experiments)

Table 3. Results for Prediction of J_{crit} for Poly(styrene) at 110 °C and Poly(*tert*-butyl acrylate) at 118 °C using Different Monomer Loadings and Targeted $M_{n,\text{th}}$

monomer	$[M]_0$ (% w/v) ^a	conv. (%)	M_n	$M_{n,\text{th}}$	M_w/M_n	expt J_{crit}	predicted J_{crit} ^b
St	70	24.5	11 800	12 250	1.15	113	110
St	70	27.6	4900	5500	1.13	47	50
St	60	12.6	7500	7500	1.19	72	65
St	50	3.6	4550	3550	1.33	44	38
<i>t</i> -BA	45	34.8	7450	6950	1.30	58	55

^a Initial monomer loading. ^b Predicted J_{crit} is from the intersection of the theoretical $M_{n,\text{th}}$ line and the curve.

obtained values of $J_{\text{crit}} = 47$ and 113. Varying the initial St monomer loadings, 50 and 60% w/v, with $M_{n,\text{th}} = 100\,000$ and 60 000 (at 100% conv.), respectively, gave predicted $J_{\text{crit}} = 38$ and 65, which were also close to those obtained experimentally at $J_{\text{crit}} = 44$ and 72. Also, in the case of *t*-BA (Figure 7 and Table 3), excellent agreement was obtained between the prediction ($J_{\text{crit}} = 55$) and experiment ($J_{\text{crit}} = 58$) for 45% w/v *t*-BA and $M_{n,\text{th}} = 20\,000$ (at 100% conv.).

The success of this predictive approach demonstrates how J_{crit} is governed by the dependence of M_n on conversion as well as the initial monomer loading. A change in $M_{n,\text{th}}$ at a fixed initial monomer loading affects J_{crit} because it alters the composition of the continuous medium at a given M_n . For example, an increase in $M_{n,\text{th}}$ by a factor of two means that a given M_n will be reached at half the conversion of the original recipe. In other words, at this value of M_n , the remaining monomer content will be higher than that for the original recipe. This understanding, as well as the predictive approach developed, is also expected to apply equally well to other CLRP systems such as ATRP and RAFT as well as non-scCO₂ media (e.g., alcohols/water). Moreover, the above is not restricted to precipitation polymerizations but also applies to dispersion (stabilized heterogeneous) polymerizations.

The J_{crit} curves in Figures 6 and 7 are shaped in such a way that at higher initial monomer loadings, the monomer content (% w/v) of the mixture (or monomer remaining) is lower than the monomer content of the mixture at lower initial monomer loadings; that is, the curve exhibits a negative gradient ("goes back on itself"). The reason is that at a high initial monomer loading, J_{crit} is so high that very significant monomer consumption is required to reach this degree of polymerization and hence the amount of remaining monomer becomes very low. This effect is particularly strong for *t*-BA, which (under the present conditions), exhibits higher J_{crit} than St. If the $M_{n,\text{th}}$ line crosses the J_{crit} curve twice, then it is the first intersection that corresponds to J_{crit} .

Effect of Pressure on J_{crit} . Attention was next turned to how pressure influences J_{crit} during precipitation NMP in scCO₂. Polymer solubility in scCO₂ increases with increasing pressure as a result of the increase in CO₂ density^{25,27} and thus solvent power. One would therefore anticipate J_{crit} to increase with increasing pressure. Figure 8 shows J_{crit} versus pressure for SG1-mediated polymerizations in scCO₂ of St 70% w/v at 110 °C ([SG1]₀/[AIBN]₀ = 2.0, $M_{n,\text{th}} = 40\,000$ at 100% conv.) and *t*-BA 60% w/v at 118 °C ([SG1]₀/[AIBN]₀ = 2.5, $M_{n,\text{th}} = 26\,900$ at 100% conv.). For both monomers, there is a close-to-linear increase in J_{crit} with increasing pressure. The increase is quite pronounced: in the case of *t*-BA, an increase in pressure from 10 to 30 MPa leads to an increase in J_{crit} from 61 to 99. In terms of conversions at J_{crit} , this means that the system is homogeneous to 24.7 and 51.8% conversion at 10 and 30 MPa, respectively. In both cases, controlled/living character is confirmed by M_n values

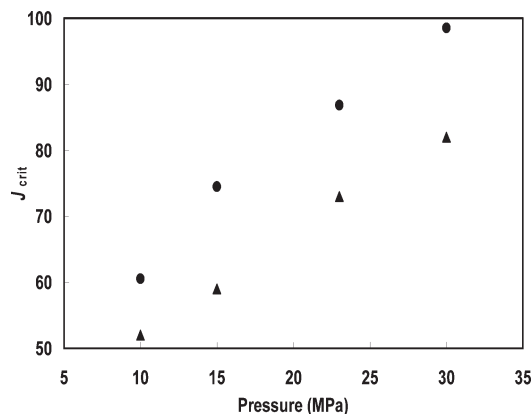


Figure 8. Plot of J_{crit} versus pressure (± 0.2 MPa) for the SG1-mediated precipitation polymerization in scCO₂ of 70% w/v St (▲) at 110 °C (using [SG1]/[AIBN] = 2.0, $M_{n,\text{th}} = 40\,000$ at 100% conv.) and 60% w/v *t*-BA (●) at 118 °C (using [SG1]/[AIBN] = 2.5, $M_{n,\text{th}} = 26\,900$ at 100% conv.).

that are reasonably close to $M_{n,\text{th}}$ and low M_w/M_n of 1.15 to 1.22 and 1.23 to 1.37 for St and *t*-BA, respectively (Tables 1 and 2).

McHugh and coworkers attributed the lower solubility of PSt relative to poly(acrylates) to its higher T_g and a very high hindrance potential for chain segment rotations giving a higher entropy penalty for CO₂ to dissolve PSt compared to poly(acrylates).²⁵ There is an overall increase in J_{crit} of 30 between 10 and 30 MPa for St, with the latter polymerization giving excellent control/living character, M_n (8550) close to $M_{n,\text{th}}$ (8800), and low M_w/M_n (1.15). At 70–80% w/v initial St loadings and the highest pressure used (30 MPa), the reaction is homogeneous over the widest conversion range (also J_{crit} is highest), which favors optimal controlled/living character at J_{crit} and beyond (as indicated by our earlier high conversion NMP precipitation polymerizations^{11,12}).

Conclusions

SG1-mediated polymerizations of St (110 °C) and *t*-BA (118 °C) were shown to proceed in a controlled/living manner from low (homogeneous) to high (heterogeneous) conversion in scCO₂ at 30 MPa. The influence of monomer-to-initiator ratio, initial monomer loading, and pressure on the critical degree of polymerization (J_{crit}) in scCO₂ has been determined. J_{crit} represents the point at which the polymerization becomes heterogeneous or polymer chains become insoluble in the continuous medium, and particle formation begins. J_{crit} increased close to linearly with increasing initial monomer loading (50 to 80% w/v and 30 to 70% w/v for St and *t*-BA, respectively) and pressure (10 to 30 MPa) for both monomers. A simple graphical approach to predict J_{crit} as a function of initial monomer loading and targeted $M_{n,\text{th}}$ ($[monomer]_0/[initiator]_0$) is presented. This predictive approach will equally apply to other CLRP systems such as ATRP and RAFT as well as non-scCO₂ media (e.g., alcohols/water). Moreover, the above is not restricted to precipitation polymerizations but also applies to dispersion polymerizations.

Acknowledgment. This publication has emanated from research work conducted with financial support from Science Foundation Ireland (08/RFP/MTR1201).

References and Notes

- (1) Kendall, J. L.; Canelas, D. A.; Young, J. L.; DeSimone, J. M. *Chem. Rev.* **1999**, *99*, 543–563.
- (2) Zetterlund, P. B.; Aldabbagh, F.; Okubo, M. *J. Polym. Sci., Part A: Polym. Chem.* **2009**, *47*, 3711–3728.

- (3) Thurecht, K. J.; Howdle, S. M. *Aust. J. Chem.* **2009**, *62*, 786–789.
- (4) Braunecker, W. A.; Matyjaszewski, K. *Prog. Polym. Sci.* **2007**, *32*, 93–146.
- (5) Zetterlund, P. B.; Kagawa, Y.; Okubo, M. *Chem. Rev.* **2008**, *108*, 3747–3794.
- (6) Cunningham, M. F. *Prog. Polym. Sci.* **2008**, *33*, 365–398.
- (7) Ryan, J.; Aldabbagh, F.; Zetterlund, P. B.; Okubo, M. *Polymer* **2005**, *46*, 9769–9777.
- (8) McHale, R.; Aldabbagh, F.; Zetterlund, P. B.; Minami, H.; Okubo, M. *Macromolecules* **2006**, *39*, 6853–6860.
- (9) McHale, R.; Aldabbagh, F.; Zetterlund, P. B.; Okubo, M. *Macromol. Rapid Commun.* **2006**, *27*, 1465–1471.
- (10) McHale, R.; Aldabbagh, F.; Zetterlund, P. B.; Okubo, M. *Macromol. Chem. Phys.* **2007**, *208*, 1813–1822.
- (11) Aldabbagh, F.; Zetterlund, P. B.; Okubo, M. *Macromolecules* **2008**, *41*, 2732–2734.
- (12) Aldabbagh, F.; Zetterlund, P. B.; Okubo, M. *Eur. Polym. J.* **2008**, *44*, 4037–4046.
- (13) Xia, J.; Johnson, T.; Gaynor, S. G.; Matyjaszewski, K.; DeSimone, J. M. *Macromolecules* **1999**, *32*, 4802–4805.
- (14) Minami, H.; Kagawa, Y.; Kuwahara, S.; Shigematsu, J.; Fujii, S.; Okubo, M. *Des. Monomers Polym.* **2004**, *7*, 553–562.
- (15) Grignard, B.; Jerome, C.; Calberg, C.; Jerome, R.; Detrembleur, C. *Eur. Polym. J.* **2008**, *44*, 861–871.
- (16) Grignard, B.; Jerome, C.; Calberg, C.; Jerome, R.; Wang, W.; Howdle, S. M.; Detrembleur, C. *Chem. Commun.* **2008**, 314–316.
- (17) Grignard, B.; Calberg, C.; Jerome, C.; Wang, W. X.; Howdle, S.; Detrembleur, C. *Chem. Commun.* **2008**, *44*, 5803–5805.
- (18) Grignard, B.; Jérôme, C.; Calberg, C.; Jérôme, R.; Wang, W.; Howdle, S. M.; Detrembleur, C. *Macromolecules* **2008**, *41*, 8575–8583.
- (19) Thurecht, K. J.; Gregory, A. M.; Wang, W.; Howdle, S. M. *Macromolecules* **2007**, *40*, 2965–2967.
- (20) Gregory, A. M.; Thurecht, K. J.; Howdle, S. M. *Macromolecules* **2008**, *41*, 1215–1222.
- (21) Zong, M. M.; Thurecht, K. J.; Howdle, S. M. *Chem. Commun.* **2008**, *45*, 5942–5944.
- (22) Lee, H.; Terry, E.; Zong, M.; Arrowsmith, N.; Perrier, S.; Thurecht, K. J.; Howdle, S. M. *J. Am. Chem. Soc.* **2008**, *130*, 12242–12243.
- (23) Cuervo-Rodriguez, R.; Bordegé, V.; Fernández-Monreal, M. C.; Fernández-García, M.; Madruga, E. L. *J. Polym. Sci., Part A: Polym. Chem.* **2004**, *42*, 4168–4176.
- (24) Guan, Z.; Combes, J. R.; Menciloglu, Y. Z.; DeSimone, J. M. *Macromolecules* **1993**, *26*, 2663–2669.
- (25) Rindfleisch, F.; DiNoia, T. P.; McHugh, M. A. *J. Phys. Chem.* **1996**, *100*, 15581–15587.
- (26) Arita, T.; Beuermann, S.; Buback, M.; Vana, P. *e-Polym.* **2004**, *003*, 1–14.
- (27) Sadowski, G. Phase Behaviour of Polymer Systems in High-Pressure Carbon Dioxide. In *Supercritical Carbon Dioxide in Polymer Reaction Engineering*, Kemmere, M. F., Meyer, T., Eds.; Wiley-VCH: Weinheim, Germany, 2005; pp 15–35.